High levels of retinal membrane docosahexaenoic acid increase susceptibility to stress-induced degeneration[S]

Masaki Tanito,[1,*,†] Richard S. Brush,[*,†] Michael H. Elliott,[*,†] Lea D. Wicker,[*,†] Kimberly R. Henry,[*,†] and Robert E. Anderson[†,§]

Departments of Ophthalmology* and Cell Biology,[§] University of Oklahoma Health Sciences Center, Oklahoma City, Oklahoma; and Dean A. McGee Eye Institute,[†] Oklahoma City, Oklahoma

Abstract **The *fat-1* gene cloned from *C. elegans* encodes an n-3 fatty acid desaturase that converts n-6 to n-3 PUFA. Mice carrying the *fat-1* transgene and wild-type controls were fed an n-3-deficient/n-6-enriched diet [*fat-1*- safflower oil (SFO) and *wt*-SFO, respectively]. Fatty acid profiles of rod outer segments (ROS), cerebellum, plasma, and liver demonstrated significantly lower n-6/n-3 ratios and higher docosahexaenoic acid (DHA) levels in *fat-1*-SFO compared with *wt*-SFO. When mice were exposed to light stress: *1*) the outer nuclear layer (ONL) thickness was reduced; *2*) amplitudes of the electroretinogram (ERG) were lower; *3*) the number of apoptotic photoreceptor cells was greater; and *4*) modification of retinal proteins by 4-hydroxyhexenal (4-HHE), an end-product of n-3 PUFA oxidation was increased in both *fat-1*-SFO and *wt* mice fed a regular lab chow diet compared with *wt*-SFO. The results indicate a positive correlation between the level of DHA, the degree of n-3 PUFA lipid peroxidation, and the vulnerability of the retina to photooxidative stress. In mice not exposed to intense light, the reduction in DHA resulted in reduced efficacy in phototransduction gain steps, while no differences in the retinal morphology or retinal biochemistry. These results highlight the dual roles of DHA in cellular physiology and pathology.**—Tanito, M., R. S. Brush, M. H. Elliott, L. D. Wicker, K. R. Henry, and R. E. Anderson. **High levels of retinal membrane docosahexaenoic acid increase susceptibility to stress-induced degeneration.** ***J. Lipid Res.*** **2009.** 50: **807–819.**

Supplementary key words retinal light damage • fat-1 • n-3 fatty acid desaturase • 4-hydoroxynonenal (4-HNE) • 4-hydroxyhexenal (4-HHE)

Linoleic acid (18:2n-6) and α-linolenic acid (18:3n-3) are essential PUFA and therefore must be obtained from the diet (1). Docosahexaenoic acid (DHA; 22:6n-3) is a metabolite of α-linolenic acid and is more abundant in rod photoreceptor outer segments (ROS) than in any other mammalian membrane (2). Studies in rodents and monkeys have demonstrated that DHA plays an important role in retinal function (3–10). Low blood levels of DHA have been reported in patients with retinitis pigmentosa (11–13) and low ROS DHA levels were found in several different animal models of human retinal degenerations (14–16).

Animals cannot synthesize n-3 or n-6 fatty acids de novo and must rely on a dietary source of these essential fatty acids. The *fat-1* gene, cloned from *C. elegans* (17), encodes an n-6 desaturase that converts n-6 to n-3 PUFA. This transgene has been expressed in mice (18), which were found to produce n-3 PUFA when fed a diet containing only n-6 PUFA. Prior analyses of *fat-1* transgenic mice revealed elevated levels of n-3 fatty acids in total lipids of brain, liver, heart, muscle, kidney, lung, spleen, and erythrocytes, but retinas were not examined (18).

Epidemiological studies have suggested that excessive light may enhance the progression and severity of age-related macular degeneration (AMD) and some forms of retinitis pigmentosa (19, 20). Acute light exposure to rats and mice causes photoreceptor and retinal pigment epithelial cell damage (21), and apoptosis is the main pathway of light-induced cell death (22). Retinal damage caused by light exposure can be reduced by various types of antioxidants (23–27). Accordingly, oxidative stress is likely to be involved in the pathogenesis of light-induced retinal damage. Exposure of the retina to intense light causes lipid peroxidation of retinal tissues (24, 28, 29) and lipid peroxidation is propagated by free radicals, especially lipid radicals (30, 31). Thus, double bonds in PUFA are target substrates

This study was supported by grants from the National Eye Institute (EY04149, EY00871, and EY12190), National Center for Research Resources (RR17703), Research to Prevent Blindness, Inc., and the Foundation Fighting Blindness. Masaki Tanito is a recipient of a Research Fellowship from the Japan Society for the Promotion of Science (JSPS) for Young Scientists.

Manuscript received 7 April 2008 and in revised form 13 August 2008 and in re-revised form 5 November 2008.

Published, JLR Papers in Press, November 20, 2008.
DOI 10.1194/jlr.M800170-JLR200

Abbreviations: AMD, age-related macular degeneration; CBB, Coomassie Brilliant Blue R-250; DHA, docosahexaenoic acid; ERG, electroretinogram; GAPDH, glyceraldehyde-3-phosphate dehydrogenase; 4-HHE, 4-hydroxyhexenal; 4-HNE, 4-hydroxynonenal; ONL, outer nuclear layer; PDE6α, phosphodiesterase 6α; ROS, rod outer segments; SFO, safflower oil.

[1] To whom correspondence should be addressed.
e-mail: tanito-oph@umin.ac.jp

[S] The online version of this article (available at http://www.jlr.org) contains supplementary data in the form of nine tables.

to propagate oxidative stress in photoreceptors. Increases in modifications of retinal proteins by reactive aldehydes such as 4-hydroxynonenal (4-HNE) and 4-hydroxyhexenal (4-HHE), end-products of nonenzymatic oxidation of n-6 PUFA and n-3 PUFA, respectively (32), precede retinal degeneration caused by acute light exposure (33, 34). Conversely, evidence suggests that DHA can also protect retinal cells from oxidative stress (35), perhaps by acting as a precursor of the neuroprotective docosatriene, neuroprotectin D1 (36, 37).

By feeding a diet rich in linoleic acid (but deficient in n-3 PUFA), we confirmed that *fat-1* transgenic mice can synthesize and incorporate n-3 PUFA into various tissues (18) and discovered that large amounts of DHA were incorporated into photoreceptor membranes. Thus, it was possible to generate littermates with a very different PUFA composition in their ROS membranes. In the current study, we used this model to determine the effect of DHA in ROS on the susceptibility to light-induced retinal damage.

EXPERIMENTAL PROCEDURES

Antibodies

The rabbit polyclonal anti-transducin α (sc-389) and mouse monoclonal anti-glyceraldehyde-3-phosphate dehydrogenase (GAPDH) (sc-32233) antibodies were purchased from Santa Cruz Biotechnology (Santa Cruz, CA). The mouse monoclonal anti-rhodopsin (MA1-722) and anti-rhodopsin kinase (MA1-720) antibodies, and rabbit polyclonal anti-phosphodiesterase 6α (PDE6α) (PA1-720) and anti-arrestin (PA1-731) antibodies were purchased from Affinity BioReagents (Golden, CO). Mouse monoclonal anti-4-HNE-modified protein antibody (anti-4-HNE antibody) and mouse monoclonal anti-4-HHE-modified protein antibody (anti-4-HHE antibody) were purchased from NOF Corporation (Tokyo, Japan) (38). The peroxidase-linked anti-mouse IgG and anti-rabbit IgG antibodies were purchased from Amersham Biosciences (Buckinghamshire, UK).

Animal care

All procedures were carried out according to the Association for Research in Vision and Ophthalmology Statement for the Use of Animals in Ophthalmic and Vision Research and the University of Oklahoma Health Sciences Center Guidelines for Animals in Research. All protocols were reviewed and approved by the Institutional Animal Care and Use Committees of the University of Oklahoma Health Sciences Center and the Dean A. McGee Eye Institute. The breeding pairs of fat-1 transgenic mice carrying a *fat-1* gene of *Caenorhabditis elegans* and wild-type C57BL/6J were kindly provided from Dr. Jing Kang (Department of Medicine, Massachusetts General Hospital and Harvard Medical School, Boston, MA) (18). *Fat-1* C57BL/6J mice were bred onto a Balb/c background, and both C57BL/6J and Balb/c *fat-1* animals were independently utilized alongside their *fat-1* negative wild-type siblings (*wt* animals). *Fat-1* and *wt* males expressing the fat-1 gene were bred to wild-type females that, prior to breeding, had been placed on a semisynthetic modified AIN-76A diet (#180465; Dyets, Bethlehem, PA) containing 10% (*wt*/*wt*) safflower oil (SFO) (n-6/n-3 ratio of 274). Mice were born and raised under a cyclic light environment (<30 lux, 12 h on/off, 7AM–7PM) in the Dean A. McGee Eye Institute vivarium and weaned onto the SFO diet (SFO animals). In some experiments, control *wt* mice (RD animals) were fed regular lab chow (LabDiet #5001, PMI Nutrition International) (n-6/n-3 ratio of 6). Fatty acid compositions and energy of each diet are shown in **Tables 1** and **2**, respectively.

TABLE 1. Fatty acid analysis on total lipid extracts of diet

Fatty Acid	10% SFO (Dyet #180465)	Control Diet (LabDiet #5001)
Saturate		
14:0	0.2 ± 0.1	1.2 ± 0.2**
16:0	7.1 ± 1.6	21.3 ± 0.4***
18:0	2.9 ± 0.1	8.1 ± 0.0***
20:0	0.3 ± 0.0	0.3 ± 0.0
22:0	0.2 ± 0.0	0.2 ± 0.0
24:0	0.2 ± 0.1	0.1 ± 0.0
Monoenoic		
16:1	0.6 ± 0.1	2.2 ± 0.0***
18:1	15.1 ± 0.5	31.1 ± 0.1***
20:1	0.3 ± 0.1	0.7 ± 0.0**
22:1	0.1 ± 0.0	0.5 ± 0.3
24:1	0.1 ± 0.0	0.1 ± 0.0
n6		
18:2n6	72.4 ± 0.7	28.6 ± 0.0***
18:3n6	0.2 ± 0.0	none detected
20:2n6	less than 0.05	0.2 ± 0.0**
20:3n6	none detected	0.1 ± 0.0
20:4n6	none detected	0.3 ± 0.0
22:4n6	none detected	0.1 ± 0.0
22:5n6	less than 0.05	0.1 ± 0.0

SFO, safflower oil diet. Relative mole percentage (± SD; n=3) of fatty acids from total lipid extracts of lab chows. Significant differences are indicated by ** and *** for $p < 0.01$ and $p < 0.001$, respectively, between 10% safflower oil and control diets using un-paired t-test. Statistical test is not applicable if the fatty acid is not detected in either group.

Genotyping

Two mm of fresh tail snips were digested with DirectPCR tail lysis reagent (Viagen Biotech, Los Angeles, CA) containing 0.3 mg/ml of Proteinase K (Sigma, St Louis, MO) at 55°C for overnight. The lysates were incubated at 95°C for 5 min. Two μl of lysate were used per PCR reaction in Green Go Taq master mix (Promega, Fitchburg, WI). The *fat-1* transgene was detected using primers 5′-CTG-CAC-CAC-GCC-TTC-ACC-AAC-C-3′ and 5′-ACA-CAG-CAG-ATT-CCA-GAG-ATT-3′ at 0.5 μM each. The PCR product (251 bp) was visualized on a 1.25% agarose gel. RPE 65 position-450 mutation was screened using primers 5′-CAC-TGT-GGT-CTC-TGC-TAT-CTT-C-3′ and 5′-GGT-GCA-GTT-CCA-CTT-CAG-TT-3′ at 0.5 μM each with Blue Taq (Denville Scientific, Metuchen, NJ) plus 2 μl of DNA tail lysate. The PCR product (674 bp) was digested with MwoI restriction enzyme for 3 h at 37°C and ran on a 1.5% agarose gel. Bands representing the

TABLE 2. Energy of diet

	10% SFO (Dyet #180465)[a]	Control Diet (LabDiet #5001)[b]
Composition (wt/wt %)		
Fat	8.1	5.7
Protein	20.3	23.9
Carbohydrate	65.0	48.7
Energy composition (kcal/g diet)		
Fat	0.90	0.55
Protein	0.73	1.16
Carbohydrate	2.34	2.36
Gross energy (kcal/g diet)	4.0	4.1

[a] Information form DYET (Bethlehem, PA).
[b] Information from PMI Nutrition International (St Louis, MO).

leucine variant were viewed at 437 bp and 236 bp. There were no methionine variants detected in the albino *fat-1* mice.

Lipid analysis

Fatty acid profiles were analyzed in ROS, cerebellum, plasma, and liver from *fat-1*-SFO and *wt*-SFO of both C57BL/6J and Balb/c strains, and in ROS from *wt*-RD of Balb/c strain. For ROS preparations, six retinas were pooled from three mice. ROS were isolated by discontinuous sucrose density centrifugation as described (28). Purity was evaluated by SDS-PAGE. A single plasma sample was obtained by pooling the heparinized blood of three mice from each group and centrifuging at 2,000 *g* in EGTA-containing tubes to obtain at least 100 μl plasma. For ROS and plasma, total lipids were extracted following the method of Bligh and Dyer (39). For liver (100 mg wet weight) and cerebellum (50 mg wet weight), total lipids were extracted following the method of Folch, Lees, and Sloane Stanley (40). Purified lipid extracts from plasma, liver, and cerebellum were resolved into neutral lipid classes using one-dimensional TLC. Briefly, an aliquot of each extract was spotted onto 10 × 20 cm Silica Gel 60 plates (EM Science, Gibbstown, NJ). Lipid classes were resolved using a 70:30:2.3 hexane:ethyl ether:glacial acetic acid mobile phase and plates were stained with 0.05% (wt/vol) 2,7-dichlorofluorescein in 75% (v/v) methanol$_{(aq)}$; phospholipids remained at the origin of the TLC plate. Fatty acids from scraped TLC spots and from purified lipid extracts from ROS were derivatized to form fatty acid methyl esters and analyzed using gas-liquid chromatography (41). The fatty acid compositions were determined by injecting 3 μl of each sample at 250°C with a split ratio of 20:1 (10:1 for ROS) onto a DB-225ms capillary column (30 m × 0.32 mm I.D.; J and W Scientific, Folsom, CA) in an Agilent 6890N gas chromatograph with model 7683 autosampler (Agilent Technologies, Wilmington, DE). The column temperature was programmed to begin at 160°C, ramped to 220°C at 1.33°C/min, and held at 220°C for 18 min. Hydrogen carrier gas flowed at 1.6 ml/min and the flame ionization detector temperature was set to 270°C. The chromatographic peaks were integrated and processed with ChemStation® software (Agilent Technologies). Fatty acid methyl esters were identified by comparison of their relative retention times with authentic standards (NU-CHEK PREP, Elysian, MN) and relative mole percentages were calculated.

Damaging light exposure

For the damaging light exposure experiments, 6-week-old Balb/c *fat-1* and *wt* mice fed with a SFO diet (*fat-1*-SFO and *wt*-SFO, respectively) and Balb/c *wt* mice fed with a regular diet (*wt*-RD) were exposed to 3,000 lux diffuse, cool, white fluorescent light for 24 h as described previously (42) with slight modifications. All light exposures began at 8:00 AM. Drinking water was supplied by a bottle attached to the side of a clear plastic cage with a wire top, so that there was no obstruction between the light and the animal. After light exposure [light (+) animals], the mice were kept under the cyclic light environment (<30 lux, 12 h on/off, 7AM–7PM) for up to 1 wk, after which electroretinograms (ERGs) were recorded and eyes were enucleated for morphometric and biochemical analyses. Age-matched mice from three groups that were not exposed to damaging light were used as controls [light (−) animals].

Electroretinography

Single flash ERGs were recorded from light (−) and (+) animals using a Ganzfeld-type ERG recording system (UTAS-E3000, LKC Technologies Inc., Gaithersburg, MD) as described previously (43). All animals were dark-adapted for 16 h before ERGs were recorded. After anesthesia was induced by intramuscular injection of a mixture of Ketamine (120 mg/kg) and xylazine (6 mg/kg), the pupils were dilated with 0.5% tropicamide and 0.5% phenylephrine hydrochloride eye drops (Santen Pharmaceutical, Osaka, Japan). Gold electrodes were placed on both eyes. An identical reference electrode was placed in the mouth and a ground electrode was placed on the tail. A single 10 msec flash of light (25 dB) from a halogen source was used as the stimulus. The a- and b-wave amplitudes recorded from both the right and the left eyes were averaged for each animal.

To determine the effects of n-3 PUFA on phototransduction efficiency, a series of scotopic ERG responses resulting from sequential single flashes from 0.4 to 3.4 log scot td-s in 0.3 log steps (1 min recovery between flashes) was recorded from Balb/c *fat-1*-SFO, *wt*-SFO, and *wt*-RD mice using an Espion ERG recording system (Diagnosys, Littleton, MA) (42). The leading edge of the a-wave was fit by a computational model of phototransduction activation (44) with an algorithm kindly provided by Dr. David G. Birch (Retina Foundation of the Southwest, Dallas, TX) using Matlab software (MathWorks, Natick, MA). This model is described by the equation: $P3(i,t) = [1 - \exp(-i \cdot S(t - t_d))(2)]R_{mp3}$ for $t > t_d$. The amplitude of P3 (the sum of individual rod responses) is a function of flash intensity (i) and time (t) after the flash onset. S is a sensitivity parameter (an indicator of phototransduction gain) that scales i. R_{mp3} is the maximum response and t_d is a brief delay (45).

Preparation of retinal samples for morphometry and biochemistry

To prepare retinal samples, mice were anesthetized using an intraperitoneal injection of Ketamine (120 mg/kg) and xylazine (6 mg/kg), perfused through the left cardiac ventricle with ice-cold PBS (pH 7.4) to wash out the blood, and enucleated. For morphometry, enucleated eyes were fixed with 4% paraformaldehyde containing 20% isopropanol, 2% trichloroacetic acid, and 2% zinc chloride for 24 h at room temperature, and embedded in paraffin (43). For biochemistry, cornea and lens were removed from enucleated eyes and retinas were separated from each eyecup. Retinal extracts were prepared by sonicating in a radioimmunoprecipitation buffer (Upstate, Lake Placid, NY) containing a protease inhibitor cocktail (Upstate), 1 mM dithiothreitol (BioRad, Hercules, CA), 2 mM diethylenetriaminepentaacetic acid (Sigma), and 100 μM butylated hydroxytoluene (Sigma), and centrifuging at 10,000 *g* for 15 min at 4°C to collect the supernatants (33). Four retinas from two mice were pooled for each preparation.

Morphometry

The outer nuclear layer (ONL) thickness was measured in retinal sections as described previously (43). Paraffin-embedded sections (4 μm thick) containing the whole retina, including the optic disc, were cut along the vertical meridian of each eyeball and stained with hematoxylin and eosin. For each section, digitized images of the entire retina were captured using an Eclipse E800 digital imaging system (Nikon, Tokyo, Japan) at 4× magnification with 1,300 × 1,030 pixels. To cover the entire retina, two images were obtained from each section. The ONL thickness was measured at 0.25, 0.5, 0.75, 1, 1.25, and 1.5 mm superior and inferior to the optic nerve head and at the periphery 100 μm from the inferior and superior edges of the retina, using Image J 1.32j software (available at http://rsb.info.nih.gov/ij/) that was developed by Wayne Rasband (National Institutes of Health, Bethesda, MD). Thickness values obtained from the right, and the left eyes were averaged for each animal.

TUNEL was performed on paraffin-embedded sections using an Apoptag Peroxidase In Situ Apoptosis Detection Kit (Chemicon, Temecula, CA) according to the manufacturer's instructions.

The chromogen-3′,3′-diaminobenzidine (Dako, Carpenteria, CA) was used. Terminal deoxynucleotidyl transferase enzyme was omitted in the negative controls.

Western dot blot analysis

Western dot blot analysis was performed as previously described (33) with slight modification. To eliminate the endogenous mouse immunoglobulins in retinal samples, retinal extracts were incubated with agarose-conjugated protein A/G (sc-2003, Sigma) at 4°C for 16 h, centrifuged at 1,000 *g* for 5 min at 4°C, and the supernatants collected. Equal aliquots (5 μg) of whole retinal protein were applied to a 96-well dot blot apparatus (BioRad) and then transferred to a polyvinylidene difluoride membrane (Millipore, Bedford, MA) by vacuum filtration. Equivalent sample loading was monitored by Coomassie Brilliant Blue R-250 (CBB) staining of a membrane loaded in parallel. After blocking with 10% nonfat dry milk for 30 min at room temperature, the membrane was incubated with the anti-4-HNE antibody (1:5,000) or the anti-4-HHE antibody (1:5,000) for 1 h at room temperature, followed by incubation with peroxidase-linked anti-mouse IgG antibody (1:5,000) for 1 h at room temperature. Chemiluminescence was developed with a SuperSignal West Dura Extended Duration Substrate (Pierce Biotechnology, Rockford, IL) and detected with a digital imaging system (IS4000R, Kodak, New Haven, CT). Care was taken to ensure that the intensities of the detected spots were within the linear range of the camera and that no pixels were saturated. The intensities of the dots stained with CBB, anti-4-HNE, and anti-4-HHE were determined using Image J 1.32j software. Coefficient of variance (CV) of this method was calculated as 12.7 ± 7.3% (mean ± SD) based on analysis of quadruplicate spots of six independent samples (33).

SDS-PAGE and Western blotting

Western blotting was performed as previously described with slight modifications (46, 47). After protein concentrations were determined using the DC protein assay kit (BioRad), equal aliquots (20 μg) of protein samples were applied to 4–15% gradient SDS-PAGE gels (BioRad) and electrophoretically separated. The gels were stained with CBB or electrophoretically transferred to polyvinylidene difluoride membranes (Millipore) and blocked with 10% nonfat dry milk for 1 h at room temperature. The membranes were incubated with anti-rhodopsin (1:2000), anti-transducin α (1:1000), anti-PDE6α (1:1000), anti-arrestin (1:1000), anti-rhodopsin kinase (1:1000), or anti-GAPDH (1:2000) antibodies for 16 h at 4°C. The membranes were incubated with peroxidase-linked anti-mouse IgG antibody (1:5000) for rhodopsin, rhodopsin kinase, and GAPDH, or with the peroxidase-linked anti-rabbit IgG antibody (1:5000) for transducin α, PDE6α, and arrestin for 1 h at room temperature. Chemiluminescence signals were developed as described for the Western dot blot experiments.

Rhodopsin assay

Mice were dark-adapted overnight and killed under dim red light by carbon dioxide asphyxiation. Both eyes were removed and homogenized in buffer containing 10 mM Tris (pH 7.4), 150 mM NaCl, 1 mM EDTA, 2% (wt/vol) octylglucoside, and 50 μM hydroxylamine. Homogenates, maintained in dim red light, were centrifuged at 16,000 *g* and the soluble fractions were scanned from 270–800 nm in an Ultrospec 3,000 UV/Vis spectrophotometer (GE Healthcare, Piscataway, NJ). The samples were subsequently bleached under room light for 15 min and scanned again. The difference in absorbance at 500 nm between pre and postbleached samples was used to determine rhodopsin content using a molar extinction coefficient of 42,000 M^{-1} (48).

RESULTS

Changes of fatty acid composition in *fat*-1 animals

We analyzed fatty acid compositions in various tissues such as ROS, cerebellum, plasma, and liver of *wt*-SFO and *fat-1*-SFO from both Balb/c and C57BL/6J strains. **Fig. 1** shows the summarized data of the n-6/n-3 ratios of each tissue (Figure 1A–D) and the polyunsaturated fatty acid levels in ROS (Fig. 1E) in the Balb/c strain. **Table 3** shows the entire data of fatty acid analysis in ROS from both Balb/c and C57BL/6J strains. A complete data set of fatty acid analysis in each tissue other than ROS from both strains is provided in supplementary Tables I–IX. When animals were maintained on a 10% SFO diet deficient in n-3 and enriched in n-6 PUFA, *fat-1* transgenic animals (*fat-1*-SFO) showed significantly elevated levels of total n-3 PUFA and lower levels of total n-6 PUFA compared with *wild-type* siblings (*wt*-SFO) for each tissue analyzed from both mouse strains. In ROS, the n-6/n-3 ratios of *wt*-SFO and *fat-1-SFO* were 1.6 and 0.2, respectively, for the Balb/c strain (Fig. 1A) and 2.6 and 0.2, respectively, for the C57BL/6J strain (Table 3). When *wild-type* Balb/c animals were maintained on a regular lab chow diet (*wt*-RD), the n-6/n-3 ratio was 0.2 in ROS (Fig. 1A). The *fat-1*-SFO in both strains had significantly higher percentages of 20:5n-3, 22:5n-3, and 22:6n-3, and significantly lower percentages of 20:4n-6, 22:4n-6, and 22:5n-6, compared with the *wt*-SFO siblings, in ROS (Fig. 1E) (Table 3) and other tissues (supplementary Tables I–IX). Notably, the increase of 22:6n-3 (DHA) in the *fat-1*-SFO compared with the *wt*-SFO siblings was greater in ROS (Fig. 1E) (Table 3) than other tissues (supplementary Tables I–IX) in both strains. There was no significant difference in the percentage of 18:2n-6 (the primary fat constituent of the diet, Table 1) or in the ratios of saturated fatty acid/PUFA between *fat-1*-SFO and *wt*-SFO in either background. The results indicate that expression of the *fat-1* transgene dramatically alters the fatty acid composition of ROS and other tissues in mice fed an n-3-deficient diet, resulting in significantly lower n-6/n-3 ratios and higher DHA levels.

Effect of fatty acid composition on light-induced retinal degeneration

Retinal function and morphology were examined in Balb/c *wt*-SFO, *fat-1*-SFO, and *wt*-RD following exposure to damaging light [light (+)]. Controls were not exposed [light (−)]. Representative ERG responses are shown in **Fig. 2A**. In light (−) animals, amplitudes of ERG a- and b-waves were not significantly different among the three groups [Fig. 2B, light (−)]. However, in light (+) animals 7 days after light exposure, ERG a- and b-waves were significantly lower in *fat-1*-SFO and *wt*-RD groups compared with those in the *wt*-SFO group. Retinal morphology was identical among the three groups in light (−) animals [**Fig. 3A**, light (−)], whereas it was different in *fat-1*-SFO and *wt*-RD compared with *wt*-SFO in light (+) animals [Fig. 3A, light (+)]. There was a loss of rod nuclei and shortening of ROS length in all three groups, the *wt*-SFO mice being the least affected. The ONL thickness measurements support the

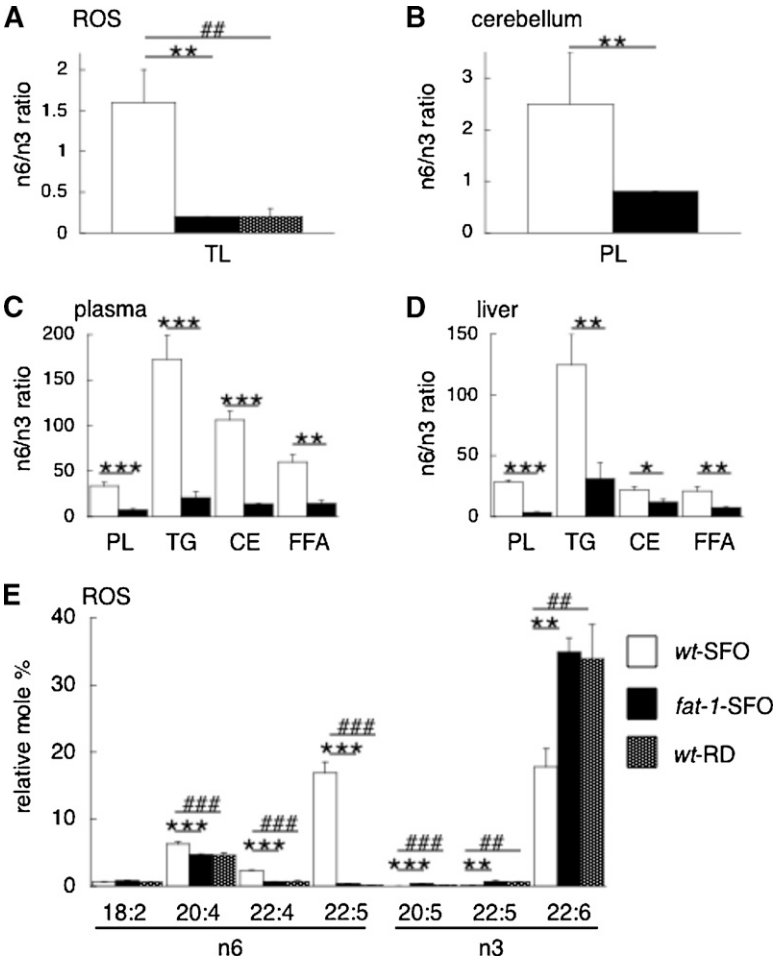

Fig. 1. Fatty acid composition of tissues from Balb/c *fat-1* and *wt* mice fed an n-3 PUFA-deficient/n-6 PUFA-rich diet, and *wt* mice fed a regular lab chow diet. A–D: The n-6/n-3 PUFA ratios of lipids from the rod outer segments (ROS) (A), cerebellum (B), plasma (C), and liver (D) of Balb/c *fat-1* transgenic mice [*fat-1* safflower oil (SFO)] and wild-type siblings (*wt*-SFO) both fed a SFO diet, and from the ROS (A) of Balb/c wild-type siblings fed a regular lab chow diet (*wt*-RD). E: Relative mole percentages of n-3 and n-6 PUFA from total lipid extracts of ROS of Balb/c *fat-1*-SFO, *wt*-SFO, and *wt*-RD. The mean ± SD is shown (n = 3) in bar graphs. Significant differences are indicated by *, **, and *** for $P < 0.05$, $P < 0.01$, and $P < 0.001$, respectively, between *fat-1*-SFO and *wt*-SFO, and by $^{\#}$, $^{\#\#}$, and $^{\#\#\#}$ for $P < 0.01$, $P < 0.01$, and $P < 0.001$, respectively, between *wt*-RD and *wt*-SFO, using a multivariant ANOVA followed by Neuman-Keuls's posthoc test. CE, cholesterol ester; FFA, free fatty acid; PL, phospholipid; ROS, rod outer segments; TL, total lipid; TG, triglyceride.

morphological findings; ONL thickness was identical among the three light (−) groups [Fig. 3B, light (−)], whereas it was significantly reduced in *fat-1*-SFO and *wt*-RD compared with *wt*-SFO light (+) animals [Fig. 3B, light (+)].

The extent of cell death in the different groups was determined by TUNEL assay. In light (−) animals, no TUNEL positive cells were observed in any retinal sections from the three groups [**Fig. 4**, light (−)]. However, in light (+) animals, larger numbers of TUNEL positive ONL cell nuclei were observed in retinal sections from *fat-1*-SFO and *wt*-RD groups compared with those from *wt*-RD [Fig. 4, light (+); insets]. These results clearly indicate that *wt*-SFO mice are much more resistant to light-induced retinal photoreceptor cell apoptosis and subsequent retinal degeneration than *fat-1*-SFO mice. This decreased sensitivity may be derived from changes in tissue n-6/n-3 ratio, as the retinal protection in *wt*-SFO was not observed in *wt*-RD mice.

Levels of lipid aldehyde-modified proteins in retinal tissues

The levels of proteins modified by 4-HNE and 4-HHE, reactive aldehydes derived from nonenzymatic oxidation of n-6 and n-3 PUFAs, respectively, were tested in Balb/c *wt*-SFO, *fat-1*-SFO, and *wt*-RD retinas from light (−) and light (+) animals by Western dot blot and densitometric analyses of total retinal lysates. In light (−) animals, the levels of proteins modified by 4-HNE (**Fig. 5A, B**) [4-HNE, light (−)] and 4-HHE (Fig. 5A, B) [4-HHE, light (−)] were not different among the three groups. In light (+) animals, the levels of 4-HNE protein modifications increased significantly in all three groups compared with the corresponding light (−) animals, but no differences were detected between the three light-exposed groups (Fig. 5A, B) [4-HNE, light (+)]. However, in light (+) animals, the levels of 4-HHE protein modification increased significantly in *fat-1*-SFO and *wt*-RD groups compared with corresponding light (−) animals, whereas, no significant increase was observed between light (−) and light (+) animals in the *wt*-SFO group. These results indicate that damaging light exposure up-regulates the formation of these biologically active aldehydes in the retina, but does not elevate 4-HHE levels in mice with high retinal n-6/n-3 ratios.

Effect of fatty acid composition on the phototransduction cascade

To determine the effect of n-6/n-3 ratios on the efficiency of phototransduction, the leading edge of ERG a-wave responses were fit to a computational model of phototransduction activation (**Fig. 6**). Representative ERG responses to increasing white flash stimuli in the Balb/c *wt*-SFO, *fat-1*-

TABLE 3. Fatty acid analysis on total lipid extracts of ROS

	Balb/c			C57/BL6J	
Fatty Acid	*wt*-SFO	*fat-1*-SFO	*wt*-RD	*wt*-SFO	*fat-1*-SFO
Saturate					
14:0	0.3 ± 0.0	0.3 ± 0.0	0.3 ± 0.0	0.4 ± 0.0	0.4 ± 0.0
16:0	20.6 ± 0.5	21.9 ± 1.1	21.8 ± 1.5	21.3 ± 0.7	20.4 ± 1.2
18:0	24.7 ± 0.7	24.5 ± 0.9	25.6 ± 1.2	22.9 ± 1.2	23.0 ± 0.3
20:0	0.2 ± 0.0	0.2 ± 0.0	0.2 ± 0.0	0.2 ± 0.0	0.2 ± 0.0
22:0	0.1 ± 0.0	0.1 ± 0.0	0.1 ± 0.0	0.1 ± 0.0	0.1 ± 0.0
24:0	less than 0.05	less than 0.05	less than 0.05	less than 0.05	less than 0.05
Monoenoic					
16:1	0.4 ± 0.0	0.4 ± 0.0	0.4 ± 0.0	0.5 ± 0.0	0.5 ± 0.1
18:1	6.2 ± 0.3	6.7 ± 0.3	7.9 ± 1.0	6.5 ± 0.4	8.0 ± 0.7
20:1	0.2 ± 0.0	0.2 ± 0.0	0.2 ± 0.0	0.2 ± 0.0	0.2 ± 0.0
22:1	0.6 ± 0.1	0.7 ± 0.2	0.3 ± 0.1#	0.1 ± 0.0	0.1 ± 0.0
24:1	less than 0.05	0.1 ± 0.0	less than 0.05	less than 0.05	less than 0.05
n6					
18:2n6	0.7 ± 0.0	0.8 ± 0.1	0.6 ± 0.1	0.9 ± 0.1	0.9 ± 0.1
18:3n6	0.1 ± 0.0	less than 0.05	less than 0.05	0.1 ± 0.0	0.1 ± 0.0
20:2n6	0.4 ± 0.0	0.3 ± 0.0	1.0 ± 0.8	0.6 ± 0.0	0.4 ± 0.0**
20:3n6	0.3 ± 0.0	0.3 ± 0.0	0.3 ± 0.0	0.5 ± 0.1	0.4 ± 0.0
20:4n6	6.3 ± 0.3	4.7 ± 0.1***	4.6 ± 0.4###	7.1 ± 0.2	5.2 ± 0.4**
22:4n6	2.3 ± 0.1	0.7 ± 0.0***	0.7 ± 0.1###	3.0 ± 0.2	0.8 ± 0.1***
22:5n6	16.9 ± 1.6	0.4 ± 0.0***	0.1 ± 0.0###	20.8 ± 1.8	0.4 ± 0.1***
n3					
18:3n3	0.1 ± 0.0	0.1 ± 0.0	0.3 ± 0.3	0.1 ± 0.0	0.1 ± 0.0
20:5n3	less than 0.05	0.4 ± 0.0***	0.2 ± 0.0###	less than 0.05	0.2 ± 0.1**
22:5n3	0.2 ± 0.0	0.7 ± 0.0**	0.6 ± 0.1##	0.1 ± 0.0	0.8 ± 0.1***
22:6n3	17.8 ± 2.7	34.9 ± 2.1**	33.9 ± 5.1##	13.1 ± 1.8	36.8 ± 2.4***
n6/n3	1.6 ± 0.4	0.2 ± 0.0**	0.2 ± 0.1##	2.6 ± 0.5	0.2 ± 0.0***
Saturate/PUFA	1.0	1.1	1.1	1.0	1.0

ROS, rod outer segments; wt-SFO, wild-type mice fed with a safflower oil diet; fat-1-SFO, fat-1 transgenic mice fed with a safflower oil diet; wt-RD, wild-type mice fed with a regular lab chow diet. Relative mole percentages (±SD; n = 3–5) of fatty acids from total lipid extracts of ROS from Balb/c and C57 BL/6J strains.

Significant differences are indicated by *, **, and *** for $P < 0.05$, $P < 0.01$, and $P < 0.001$, respectively, between fat-1-SFO and wt-SFO; and by #, ##, and ### for $P < 0.01$, $P < 0.01$, and $P < 0.001$, respectively, between wt-RD and wt-SFO, using a multivariant ANOVA followed by Neuman-Keuls's posthoc test.

SFO, and *wt*-RD are shown in Fig. 6A, B, and C, respectively. The derived sensitivity (S) parameter, a measure of the amplification steps of the phototransduction cascade, was significantly higher (Fig. 6D) and the implicit time of the a-wave at lower flash intensities was significantly shorter (Fig. 6E) in *fat-1*-SFO and *wt*-RD compared with that of *wt*-SFO, whereas the derived log maximal a-wave amplitude was identical among three groups (data not shown), consistent with the lack of a-wave amplitude changes observed in the light (−) group presented in Fig. 2B. These results reinforce the idea that there is a relationship between the sensitivity of the photocascade and DHA levels.

To determine whether the decreased sensitivity observed in *wt*-SFO mice is due to alterations in the protein composition of ROS, we examined ROS protein profiles by SDS-PAGE. There were no observable differences in ROS protein profiles between *wt*-SFO and *fat-1*-SFO in either Balb/c (**Fig. 7A**) or C57BL/6J (data not shown). Furthermore, Western blot analyses of several phototransduction-related proteins revealed no differences in the expression levels of any of them in *wt*-SFO, *fat-1*-SFO, or *wt*-RD in Balb/c strain (Fig. 7B). Finally, we found no differences in bleachable rhodopsin content in *wt*-SFO and *fat-1*-SFO regardless of background (Fig. 7C). These results suggest that the observed differences in phototransduction efficiency among groups are not due to differences in the content of photoactivatable rhodopsin or in the expression levels of other phototransduction-related molecules.

DISCUSSION

The *fat-1* transgene encodes an n-3 fatty acid desaturase that converts n-6 to n-3 PUFA (17, 18). In this study, we demonstrated that expression of the *fat-1* transgene enables mice fed an n-3-deficient diet to endogenously synthesize and incorporate n-3 fatty acids into ROS membranes (as well as other tissues), resulting in significantly lower n-6/n-3 ratios (Fig. 1) (Table 3) (see supplementary Tables I–IX). The fatty acid compositions of *wt* mice fed the SFO diet were similar to those reported in previous studies, with increases in 22:5n-6 offsetting the reduction in 22:6n-3 (3, 10, 49). This offset was largely responsible for the increase in the n-6/n-3 ratios observed in *wt*-SFO animals and is indicative of dietary deficiency of 22:6n-3. This is most evident in the ROS and cerebellum, which have the highest levels of 22:6n-3 (DHA). No changes were observed in the saturated fatty acid/PUFA ratios in any tissues.

In general, there were no great differences in the fatty acid compositions of the various tissues from the C57BL/6J and Balb/c mice. However, one exception was the level of 22:6n-3 in the ROS and cerebellum of the albino mice,

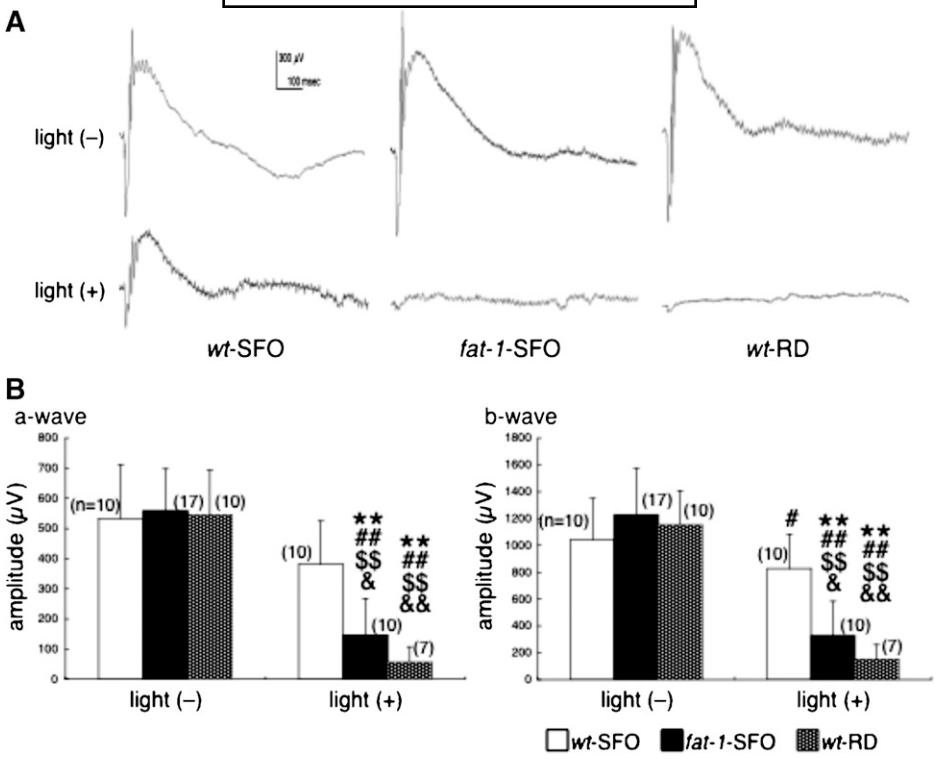

Fig. 2. Measurement of retinal function by electroretinography (ERG). A: Representative ERG recordings from wild-type mice fed a SFO diet (*wt*-SFO), *fat-1* transgenic mice fed a SFO diet (*fat-1*-SFO), and wild-type mice fed a regular diet (*wt*-RD) with [light (+)] and without [light (−)] damaging light exposure. The experiments were performed on the Balb/c strain. B: ERG a-wave (left panel) and b-wave (right panel) amplitudes (mean ± SD) are shown. Significant differences are indicated by ** for $P < 0.01$ against light (−) *wt*-SFO; by $^{\#}$ and $^{\#\#}$ for $P < 0.05$ and $P < 0.01$, respectively, against light (−) *fat-1*-SFO; by $^{\$\$}$ for $P < 0.01$ against light (−) *wt*-RD; and $^{\&}$ and $^{\&\&}$ for $P < 0.05$ and $P < 0.01$, respectively, against light (+) *wt*-SFO, using a one-way ANOVA followed by Scheffe's posthoc test. The number of animals analyzed is indicated in each graph.

where the reduction of 22:6n-3 and concomitant increase in 22:5n-6 were less pronounced in the albino than in the pigmented mice. We and others (49, 50) have previously shown that the retina conserves n-3 PUFA during n-3 deficiency. There is efficient recycling of 22:6n-3 between the retina and the retinal pigment epithelium that makes it difficult to deplete the 22:6n-3 from an adult animal. It appears that the recycling may be more efficient in the Balb/c mice, because they retained higher levels of 22:6n-3 in the *wt* retinas.

The ability of the *fat-1* transgenic mice to synthesize n-3 PUFA from n-6 PUFA provides a viable alternative to studies that would normally involve two diets. As indicated by our data, the fatty acid composition of ROS membranes from *fat-1*-SFO mice was indistinguishable from wild-type mice fed standard lab chow. Typically, to study the effects of n-3 PUFA and DHA in an animal model, two isocaloric diets are required: one experimental diet rich in n-3 PUFA and another control diet devoid of n-3 PUFA. Preparation of the n-3 rich diet requires replacement of n-6 PUFA with n-3 PUFA to maintain the isocaloric quality. Under these circumstances, it could be argued that any experimental differences could be the result of either an increase in n-3 PUFA or a decrease in n-6 PUFA in the diet. The *fat-1* transgenic mouse is able to increase n-3 PUFA, including DHA, in ROS and other tissues without introducing the variable of another diet. One caveat for optimizing the reduction in 22:6n-3 in brain and retina is that the female should be wild-type and the male should carry the *fat-1* transgene, and that the SFO diet be initiated before the mice are bred. This will ensure that n-3 PUFA deprivation will begin in utero, which will lead to a much greater reduction in DHA in wild-type animals compared with mice started on the diet at weaning.

In animals not exposed to light, the reduction in n-3 PUFA yielded no difference in the morphology of rod photoreceptor cells, as evidenced by the same number of photoreceptor nuclei in the ONL of all three groups in Balb/c (Fig. 3) and C57BL/6J (data not shown) strains. The rhodopsin content of the *wt*-SFO and *fat-1*-SFO in both strains was the same, and there were no apparent differences in the protein profiles as determined by SDS-PAGE and by Western blots (Fig. 7). This is in agreement with earlier studies showing that n-3 deficiency did not affect rhodopsin content (3, 10), but at odds with one study showing an increase in rhodopsin levels with n-3 deficiency (51). As this latter study compared two different diets, it is possible that differences in rhodopsin levels resulted from a difference in the diets independent of n-3 deficiency. In the current experiments, mice were reared on the same diet

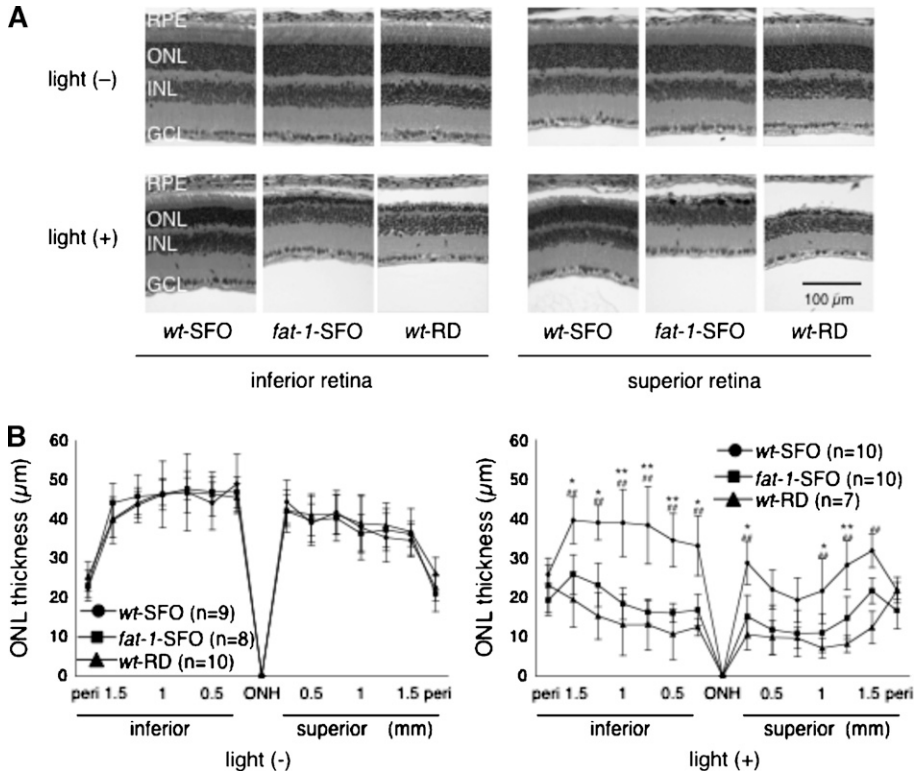

Fig. 3. Quantification of the outer nuclear layer (ONL) thickness. A: Representative hematoxylin and eosin staining of retinal sections at 0.5–1.0 mm inferior (left panels) and superior (right panels) to the optic nerve head from *wt*-SFO, *fat-1*-SFO, and *wt*-RD with [light (+)] and without [light (−)] damaging light exposure. The experiments were performed on the Balb/c strain. In the light (+) group, eyes were enucleated 7 days after the damaging light exposure. GCL, ganglion cell layer; INL, inner nuclear layer; ONL, outer nuclear layer; RPE, retinal pigment epithelium. B: ONL thickness (mean ± SD) in *wt*-SFO, *fat-1*-SFO, and *wt*-RD with (right panel) and without (left panel) damaging light exposure. Significant differences are indicated by * and ** for $P < 0.05$ and $P < 0.01$, respectively, between *wt*-SFO and *fat-1*-SFO, and by $^{\#\#}$ for $P < 0.01$ between *wt*-SFO and *wt*-RD, using a one-way ANOVA followed by Scheffe's posthoc test. The number of animals analyzed is indicated in each graph.

so this variable is removed from our analyses. Thus, the dramatic changes in fatty acid composition were not accompanied by any measurable changes in retinal morphology or chemistry.

The functional and morphological analyses in the light-damage experiments revealed that retinas from animals with low n-6/n-3 ratios (i.e., *fat-1*-SFO and *wt*-RD mice) were severely damaged (Figs. 2–4). Several previous stud-

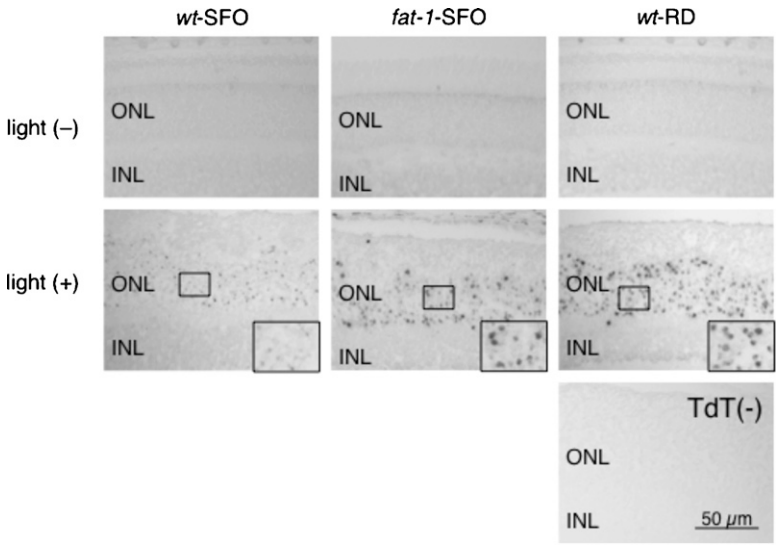

Fig. 4. TUNEL staining of retinal sections. Representative TUNEL staining of retinal sections at 0.5–1.0 mm superior to the optic nerve head from *wt*-SFO, *fat-1*-SFO, and *wt*-RD without [light (−)] and with [light (+)] damaging light exposure are shown. The experiments were performed on the Balb/c strain. In the light (+) group, eyes were enucleated immediately after damaging light exposure for 24 h. ONL, outer nuclear layer; and INL, inner nuclear layer. Terminal deoxynucleotidyl transferase (−), no terminal deoxynucleotidyl transferase enzyme on the same section of light (+) *wt*-RD as a negative control.

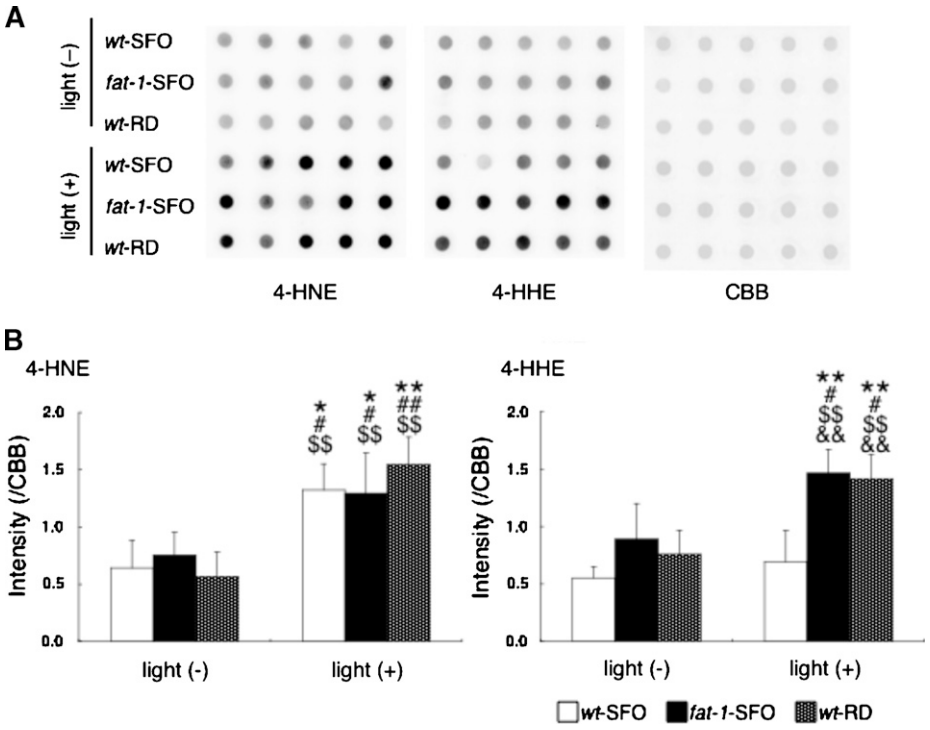

Fig. 5. Western dot blots of 4-hydroxynonenal (4-HNE) and 4-hydroxyhexenal (4-HHE) in retinal samples. A: Blots of protein modifications by 4-HNE (left panel), protein modifications by 4-HHE (center panel), and Coomassie Brilliant Blue R-250 (CBB) staining served as a loading control (right panel) in total retinal lysates from *wt*-SFO, *fat-1*-SFO, and *wt*-RD with [light (+)] and without [light (−)] damaging light exposure. The experiments were performed on the Balb/c strain. In the light (+) group, eyes were enucleated immediately after 24 h of damaging light exposure. Five independent total retinal protein preparations in each of three groups are represented (pooled four retinas from two mice are used for each preparation). B: Densitometric analysis of blots in (A). The mean (±SD) densities standardized using CBB staining are shown for light (−) and light (+) animals in each three groups (n = 5 in each group). Significant differences are indicated by * and ** for $P < 0.05$ and $P < 0.01$, respectively, against light (−) *wt*-SFO; by $^{\#}$ and $^{\#\#}$ for $P < 0.05$ and $P < 0.01$, respectively, against light (−) *fat-1*-SFO; by $^{\$\$}$ for $P < 0.01$ against light (−) *wt*-RD; and by $^{\&\&}$ for $P < 0.01$ against light (+) *wt*-SFO, using a one-way ANOVA followed by Scheffe's posthoc test.

ies using dietary deprivation of n-3 PUFA in albino rats have reported a positive relationship between n-3-PUFA levels and susceptibility to light damage (51–53). However, the difference in severity of retinal damage among the groups in our study was much larger than those in previous reports. This could be due to the greater difference in DHA levels between the groups in our study or to the species tested. Also, all of the published studies testing the role of DHA in the susceptibility of photoreceptors to light damage have been done on rats. We used albino mice in the light damage experiments, where the sensitivity to DHA photooxidation may be greater than albino rats. Regardless of the explanation, our results strongly suggest that the levels of n-3 PUFA are related to the vulnerability of the retina to photooxidative stress.

Levels of retinal proteins modified by 4-HHE, which is derived from n-3 PUFA oxidation, increased in the *fat-1*-SFO and *wt*-RD groups with light exposure compared with light (−) animals, but was unchanged in the *wt*-SFO (Fig. 5). These results demonstrate the relationship between tissue levels of n-3 PUFA or DHA and the levels of their oxidized end products. Due to facile reactivity with histidine, cysteine, or lysine residues of proteins (32), these reactive aldehydes exhibit a variety of cytopathological effects such as inhibition of enzyme activity, inhibition of protein, RNA, and DNA synthesis, cell cycle arrest, and apoptosis (54, 55). Our earlier work suggests that modifications by lipid aldehydes on a specific set of retinal proteins are molecular events that precede light-induced photoreceptor cell apoptosis (33, 34). Collectively, with the morphological and functional analyses, current results strongly suggest the causal relationships among levels of n-3 PUFA, n-3 PUFA oxidation, and the vulnerability of the retina to photooxidative stress. Levels of retinal proteins modified by 4-HNE, which is derived from n-6 PUFA oxidation, increased only in light (+) groups, independent of diet or *fat-1* expression, in spite of the dramatic molecular replacement of 22:6n-3 with 22:5n-6 in *wt*-SFO group. Currently, the reason for this lack of direct association between the levels of n-6 PUFA, their oxidized end products, and the severity of retinal damage is unknown. This lack of direct association and possible protection of retina by n-6 PUFA against photooxidative stress could be analyzed in the future.

The long-chain PUFA DHA is more abundant in ROS than in any other mammalian membrane (2) and photoreceptors have a robust mechanism to conserve it (49). A

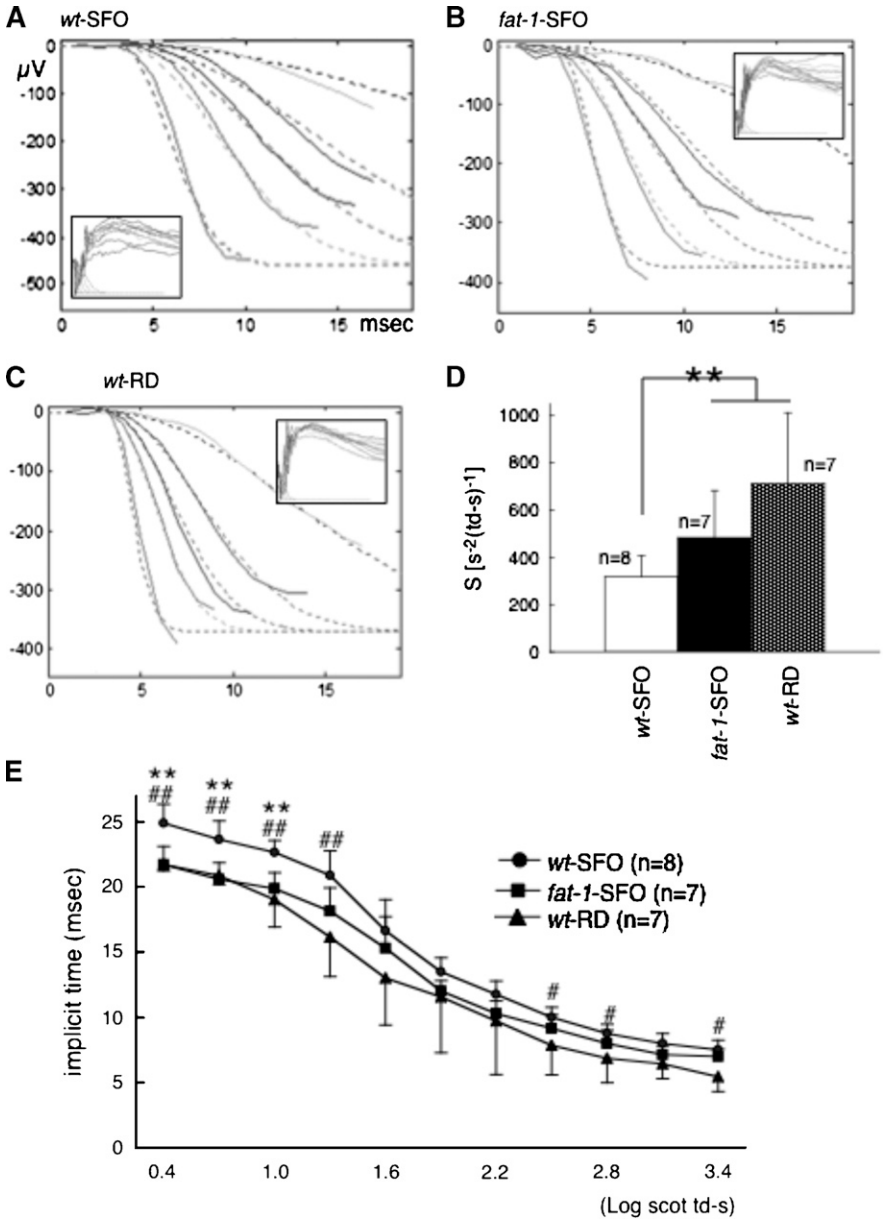

Fig. 6. Analysis of ERG a-wave. A–C: Representative ERG recordings (solid curves) and best fit of equation (dashed curves) from *wt*-SFO (A), *fat-1*-SFO (B), and *wt*-RD (C) against white flash ranging in energy from 0.4 to 3.4 log scot td-s with 0.3 log steps (insets). The experiments were performed on the Balb/c strain. Flash in energy at 0.7, 1.3, 1.6, 1.9, and 2.5 log scot td-s are used for the fit. D: The mean (±SD) of best fit sensitivity (S) parameter is shown. Significant differences are indicated by ** for $P < 0.01$ using a one-way ANOVA followed by Scheffe's posthoc test. E: The mean (±SD) of implicit time of the a-wave against sequential intensity is shown. Significant differences are indicated by ** for $P < 0.01$ between *wt*-SFO, and *fat-1*-SFO by ## for $P < 0.01$ between *wt*-SFO and *fat-1*-SFO. The number of animals analyzed is indicated in each graph.

requirement of n-3 fatty acids for optimal development of visual acuity and stereoacuity in term and preterm human infants has also been reported (56). Furthermore, we showed a number of years ago that fatty acid composition of ROS membranes is an important determinant for optimal retinal function in rodents (3, 4) and DHA deficiency results in reduction of ERG response with a-wave amplitudes affected more profoundly. Reduced maximal response amplitudes attributed to n-3 deficiency have also been observed in guinea pigs (57), monkeys (58), and in n-3-deficient preterm human infants (5). However, some studies (including the present one) did not observe significant effects of DHA deficiency on maximal ERG response amplitudes (6, 7). The reason for this discrepancy among studies reported is not clear, but the small difference in the light intensity in the vivarium, differences in the diet composition, or differences in the species might have affected the phenotype. Although we did not observe significant differences in a-wave amplitudes in nonlight-damaged animals, we did observe a significant reduction in sensitivity with lower DHA

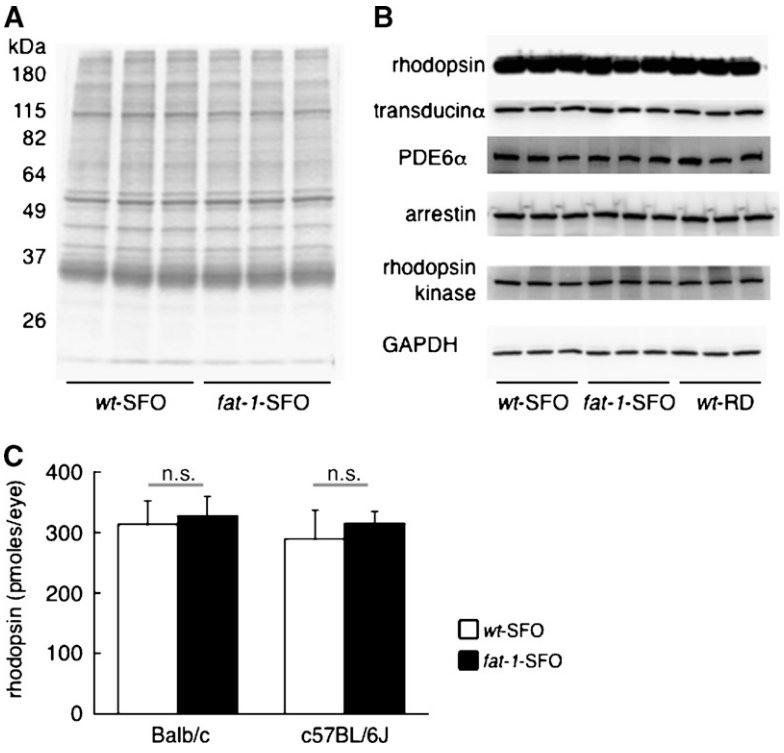

Fig. 7. SDS-PAGE, Western blots, and rhodopsin assays on retinal samples. A: SDS-PAGE of ROS proteins from Balb/c *wt*-SFO and Balb/c *fat-1*-SFO. Three independent ROS preparations in each group are represented (pooled six retinas from three mice are used for each preparation). B: Western blots against phototransduction-related molecules and glyceraldehyde-3-phosphate dehydrogenase (GAPDH) as a loading control in total retinal lysates from Balb/c *wt*-SFO, *fat-1*-SFO, and *wt*-RD. Three independent total retinal protein preparations in each of three groups are represented (pooled four retinas from two mice are used for each preparation). C: Rhodopsin content in eyes from *wt*-SFO and *fat-1*-SFO in both Balb/c and C57BL/6J strains. The mean ± SD (pmoles/eye) is shown in bar graph (n = 5 eyes from five mice in each group). The n.s. indicates no significance between groups using an unpaired *t*-test.

levels (or higher n-6/n-3 ratios) (Fig. 6), suggesting that phototransduction amplification is influenced by the DHA level and n-6/n-3 ratio. This result is supported by studies showing decreased sensitivity in n-3-deficient rats (59) and monkeys (60), and in preterm human infants (5). Decreased S parameter was reported in human retinitis pigmentosa patients (45). In addition, a-wave implicit time is slowed in mice deficient in DHA as has been observed in baboons (61). Accordingly, our results suggest a correlation between the activation and kinetics of phototransduction and the sensitivity to light damage. However, mice in which the phototransduction G-protein, transducin, has been deleted are as sensitive to bright light-induced retinal degeneration as wild-type controls, although when rhodopsin shutoff is inhibited, mice are extremely light sensitive (62). Perhaps the protection from lower DHA levels in ROS membranes results from decreased rhodopsin activation. In fact, n-3 deficiency has been shown to reduce rhodopsin activation, reduce and delay rhodopsin-transducin coupling, and decrease cGMP-phosphodiesterase activity in biochemical assays (10).

The roles of DHA in the retina are potentially conflicting in the literature. Cell-culture studies have shown that DHA protects retinal (35) and retinal pigment epithelial (36, 37) cells from oxidant stress-induced apoptosis. A diet rich in n-3 fatty acids was shown to be inversely associated with the risk for AMD (63, 64). On the basis of these and other studies, the recently undertaken AREDS II clinical trial will determine the role of DHA in the development and progression of AMD. On the other hand, DHA is implicated in retinal degenerations through its capacity to act as an oxidation substrate. Crabb et al. (65) found an increased decoration of proteins in Bruch's membrane preparations from human eyes with AMD compared with age-matched controls using a carboxyethylpyrrole antibody that recognizes protein adducts formed by peroxidation of DHA. It would be of great interest to know the correlation between levels of biologically active DHA metabolites such as neuroprotectin D1 and carboxyethylpyrrole and the relative degree of retinal degeneration in our experimental model in the future. In the present study, we provide clear evidence that *fat-1*-SFO mice are more susceptible to light damage than *wt*-SFO mice, and that the levels of DHA, the major n-3 PUFA in retina, and protein modifications by its oxidation products 4-HHE are positively related to the vulnerability. These results highlight the ying and yang roles of n-3 PUFA and DHA in retinal physiology and pathology.

The authors are grateful to Dr. Jing Kang (Department of Medicine, Massachusetts General Hospital and Harvard Medical School) for providing a bleeding pair of *fat-1* transgenic mice for this study, Dr. David G. Birch (Retina Foundation of the Southwest) for providing the algorithm program for a-wave analysis, Mark Dittmar (Dean A. McGee Eye Institute) for maintaining the animal colonies used in this study, and to Louisa J. Williams and Linda S. Boone (Dean A. McGee Eye Institute) for their excellent retinal section preparation.

REFERENCES

1. Tinoco, J. 1982. Dietary requirements and functions of alpha-linolenic acid in animals. *Prog. Lipid Res.* **21:** 1–45.
2. Fliesler, S. J., and R. E. Anderson. 1983. Chemistry and metabolism of lipids in the vertebrate retina. *Prog. Lipid Res.* **22:** 79–131.
3. Benolken, R. M., R. E. Anderson, and T. G. Wheeler. 1973. Mem-

brane fatty acids associated with the electrical response in visual excitation. *Science.* **182:** 1253–1254.
4. Wheeler, T. G., R. M. Benolken, and R. E. Anderson. 1975. Visual membranes: specificity of fatty acid precursors for the electrical response to illumination. *Science.* **188:** 1312–1314.
5. Birch, D. G., E. E. Birch, D. R. Hoffman, and R. D. Uauy. 1992. Retinal development in very-low-birth-weight infants fed diets differing in omega-3 fatty acids. *Invest. Ophthalmol. Vis. Sci.* **33:** 2365–2376.
6. Bush, R. A., A. Malnoe, C. E. Reme, and T. P. Williams. 1994. Dietary deficiency of N-3 fatty acids alters rhodopsin content and function in the rat retina. *Invest. Ophthalmol. Vis. Sci.* **35:** 91–100.
7. Jeffrey, B. G., D. C. Mitchell, R. A. Gibson, and M. Neuringer. 2002. n-3 fatty acid deficiency alters recovery of the rod photoresponse in rhesus monkeys. *Invest. Ophthalmol. Vis. Sci.* **43:** 2806–2814.
8. Mitchell, D. C., S. L. Niu, and B. J. Litman. 2003. Enhancement of G protein-coupled signaling by DHA phospholipids. *Lipids.* **38:** 437–443.
9. Anderson, R. E., and J. S. Penn. 2004. Environmental light and heredity are associated with adaptive changes in retinal DHA levels that affect retinal function. *Lipids.* **39:** 1121–1124.
10. Niu, S. L., D. C. Mitchell, S. Y. Lim, Z. M. Wen, H. Y. Kim, N. Salem, Jr., and B. J. Litman. 2004. Reduced G protein-coupled signaling efficiency in retinal rod outer segments in response to n-3 fatty acid deficiency. *J. Biol. Chem.* **279:** 31098–31104.
11. Anderson, R. E., M. B. Maude, R. A. Lewis, D. A. Newsome, and G. A. Fishman. 1987. Abnormal plasma levels of polyunsaturated fatty acid in autosomal dominant retinitis pigmentosa. *Exp. Eye Res.* **44:** 155–159.
12. Hoffman, D. R., and D. G. Birch. 1995. Docosahexaenoic acid in red blood cells of patients with X-linked retinitis pigmentosa. *Invest. Ophthalmol. Vis. Sci.* **36:** 1009–1018.
13. Hoffman, D. R., R. Uauy, and D. G. Birch. 1993. Red blood cell fatty acid levels in patients with autosomal dominant retinitis pigmentosa. *Exp. Eye Res.* **57:** 359–368.
14. Anderson, R. E., M. B. Maude, and D. Bok. 2001. Low docosahexaenoic acid levels in rod outer segment membranes of mice with rds/peripherin and P216L peripherin mutations. *Invest. Ophthalmol. Vis. Sci.* **42:** 1715–1720.
15. Anderson, R. E., M. B. Maude, M. McClellan, M. T. Matthes, D. Yasumura, and M. M. LaVail. 2002. Low docosahexaenoic acid levels in rod outer segments of rats with P23H and S334ter rhodopsin mutations. *Mol. Vis.* **8:** 351–358.
16. Bicknell, I. R., R. Darrow, L. Barsalou, S. J. Fliesler, and D. T. Organisciak. 2002. Alterations in retinal rod outer segment fatty acids and light-damage susceptibility in P23H rats. *Mol. Vis.* **8:** 333–340.
17. Spychalla, J. P., A. J. Kinney, and J. Browse. 1997. Identification of an animal omega-3 fatty acid desaturase by heterologous expression in Arabidopsis. *Proc. Natl. Acad. Sci. USA.* **94:** 1142–1147.
18. Kang, J. X., J. Wang, L. Wu, and Z. B. Kang. 2004. Transgenic mice: fat-1 mice convert n-6 to n-3 fatty acids. *Nature.* **427:** 504.
19. Cruickshanks, K. J., R. Klein, and B. E. Klein. 1993. Sunlight and age-related macular degeneration. The Beaver Dam Eye Study. *Arch. Ophthalmol.* **111:** 514–518.
20. Cideciyan, A. V., D. C. Hood, Y. Huang, E. Banin, Z. Y. Li, E. M. Stone, A. H. Milam, and S. G. Jacobson. 1998. Disease sequence from mutant rhodopsin allele to rod and cone photoreceptor degeneration in man. *Proc. Natl. Acad. Sci. USA.* **95:** 7103–7108.
21. Tytell, M., M. F. Barbe, and D. J. Gower. 1989. Photoreceptor protection from light damage by hyperthermia. *Prog. Clin. Biol. Res.* **314:** 523–538.
22. Hafezi, F., J. P. Steinbach, A. Marti, K. Munz, Z. Q. Wang, E. F. Wagner, A. Aguzzi, and C. E. Reme. 1997. The absence of c-fos prevents light-induced apoptotic cell death of photoreceptors in retinal degeneration in vivo. *Nat. Med.* **3:** 346–349.
23. Organisciak, D. T., H. M. Wang, Z. Y. Li, and M. O. Tso. 1985. The protective effect of ascorbate in retinal light damage of rats. *Invest. Ophthalmol. Vis. Sci.* **26:** 1580–1588.
24. Organisciak, D. T., R. M. Darrow, Y. I. Jiang, G. E. Marak, and J. C. Blanks. 1992. Protection by dimethylthiourea against retinal light damage in rats. *Invest. Ophthalmol. Vis. Sci.* **33:** 1599–1609.
25. Ranchon, I., M. M. LaVail, Y. Kotake, and R. E. Anderson. 2003. Free radical trap phenyl-N-tert-butylnitrone protects against light damage but does not rescue P23H and S334ter rhodopsin transgenic rats from inherited retinal degeneration. *J. Neurosci.* **23:** 6050–6057.
26. Tanito, M., M. P. Agbaga, and R. E. Anderson. 2007. Upregulation of thioredoxin system via Nrf2-antioxidant responsive element pathway in adaptive-retinal neuroprotection in vivo and in vitro. *Free Radic. Biol. Med.* **42:** 1838–1850.
27. Tanito, M., F. Li, M. H. Elliott, M. Dittmar, and R. E. Anderson. 2007. Protective effect of TEMPOL derivatives against light-induced retinal damage in rats. *Invest. Ophthalmol. Vis. Sci.* **48:** 1900–1905.
28. Wiegand, R. D., N. M. Giusto, L. M. Rapp, and R. E. Anderson. 1983. Evidence for rod outer segment lipid peroxidation following constant illumination of the rat retina. *Invest. Ophthalmol. Vis. Sci.* **24:** 1433–1435.
29. Tanito, M., Y. Yoshida, S. Kaidzu, A. Ohira, and E. Niki. 2006. Detection of lipid peroxidation in light-exposed mouse retina assessed by oxidative stress markers, total hydroxyoctadecadienoic acid and 8-iso-prostaglandin F(2alpha). *Neurosci. Lett.* **398:** 63–68.
30. De La Paz, M. A., and R. E. Anderson. 1992. Lipid peroxidation in rod outer segments. Role of hydroxyl radical and lipid hydroperoxides. *Invest. Ophthalmol. Vis. Sci.* **33:** 2091–2096.
31. Winkler, B. S., M. E. Boulton, J. D. Gottsch, and P. Sternberg. 1999. Oxidative damage and age-related macular degeneration. *Mol. Vis.* **5:** 32.
32. Uchida, K., and E. R. Stadtman. 1992. Modification of histidine residues in proteins by reaction with 4-hydroxynonenal. *Proc. Natl. Acad. Sci. USA.* **89:** 4544–4548.
33. Tanito, M., M. H. Elliott, Y. Kotake, and R. E. Anderson. 2005. Protein modifications by 4-hydroxynonenal and 4-hydroxyhexenal in light-exposed rat retina. *Invest. Ophthalmol. Vis. Sci.* **46:** 3859–3868.
34. Tanito, M., H. Haniu, M. H. Elliott, A. K. Singh, H. Matsumoto, and R. E. Anderson. 2006. Identification of 4-hydroxynonenal-modified retinal proteins induced by photooxidative stress prior to retinal degeneration. *Free Radic. Biol. Med.* **41:** 1847–1859.
35. Rotstein, N. P., L. E. Politi, O. L. German, and R. Girotti. 2003. Protective effect of docosahexaenoic acid on oxidative stress-induced apoptosis of retina photoreceptors. *Invest. Ophthalmol. Vis. Sci.* **44:** 2252–2259.
36. Mukherjee, P. K., V. L. Marcheselli, C. N. Serhan, and N. G. Bazan. 2004. Neuroprotectin D1: a docosahexaenoic acid-derived docosatriene protects human retinal pigment epithelial cells from oxidative stress. *Proc. Natl. Acad. Sci. USA.* **101:** 8491–8496.
37. Bazan, N. G. 2007. Homeostatic regulation of photoreceptor cell integrity: significance of the potent mediator Neuroprotectin D1 biosynthesized from docosahexaenoic acid. The Proctor Lecture. *Invest. Ophthalmol. Vis. Sci.* **48:** 4866–4881.
38. Toyokuni, S., N. Miyake, H. Hiai, M. Hagiwara, S. Kawakishi, T. Osawa, and K. Uchida. 1995. The monoclonal antibody specific for the 4-hydroxy-2-nonenal histidine adduct. *FEBS Lett.* **359:** 189–191.
39. Bligh, E. G., and W. J. Dyer. 1959. A rapid method of total lipid extraction and purification. *Can. J. Biochem. Physiol.* **37:** 911–917.
40. Folch, J., M. Lees, and G. H. Sloane Stanley. 1957. A simple method for the isolation and purification of total lipides from animal tissues. *J. Biol. Chem.* **226:** 497–509.
41. Morrison, W. R., and L. M. Smith. 1964. Preparation of fatty acid methyl esters and dimethylacetals from lipids with boron fluoride–methanol. *J. Lipid Res.* **5:** 600–608.
42. Tanito, M., and R. E. Anderson. 2006. Bright cyclic light rearing-mediated retinal protection against damaging light exposure in adrenalectomized mice. *Exp. Eye Res.* **83:** 697–701.
43. Tanito, M., S. Kaidzu, and R. E. Anderson. 2007. Delayed loss of cone and remaining rod photoreceptor cells due to impairment of choroidal circulation after acute light exposure in rats. *Invest. Ophthalmol. Vis. Sci.* **48:** 1864–1872.
44. Lamb, T. D., and E. N. Pugh, Jr. 1992. A quantitative account of the activation steps involved in phototransduction in amphibian photoreceptors. *J. Physiol.* **449:** 719–758.
45. Hood, D. C., and D. G. Birch. 1994. Rod phototransduction in retinitis pigmentosa: estimation and interpretation of parameters derived from the rod a-wave. *Invest. Ophthalmol. Vis. Sci.* **35:** 2948–2961.
46. Tanito, M., H. Masutani, Y. C. Kim, M. Nishikawa, A. Ohira, and J. Yodoi. 2005. Sulforaphane induces thioredoxin through the antioxidant-responsive element and attenuates retinal light damage in mice. *Invest. Ophthalmol. Vis. Sci.* **46:** 979–987.
47. Tanito, M., Y. W. Kwon, N. Kondo, J. Bai, H. Masutani, H. Nakamura, J. Fujii, A. Ohira, and J. Yodoi. 2005. Cytoprotective effects of geranylgeranylacetone against retinal photooxidative damage. *J. Neurosci.* **25:** 2396–2404.
48. Irreverre, F., A. L. Stone, H. Shichi, and M. S. Lewis. 1969. Biochemistry of visual pigments. I. Purification and properties of bovine rhodopsin. *J. Biol. Chem.* **244:** 529–536.

49. Wiegand, R. D., C. A. Koutz, A. M. Stinson, and R. E. Anderson. 1991. Conservation of docosahexaenoic acid in rod outer segments of rat retina during n-3 and n-6 fatty acid deficiency. *J. Neurochem.* **57:** 1690–1699.
50. Anderson, R. E., P. J. O'Brien, R. D. Wiegand, C. A. Koutz, and A. M. Stinson. 1992. Conservation of docosahexaenoic acid in the retina. *Adv. Exp. Med. Biol.* **318:** 285–294.
51. Bush, R. A., C. E. Reme, and A. Malnoe. 1991. Light damage in the rat retina: the effect of dietary deprivation of N-3 fatty acids on acute structural alterations. *Exp. Eye Res.* **53:** 741–752.
52. Koutz, C. A., R. D. Wiegand, L. M. Rapp, and R. E. Anderson. 1995. Effect of dietary fat on the response of the rat retina to chronic and acute light stress. *Exp. Eye Res.* **60:** 307–316.
53. Organisciak, D. T., R. M. Darrow, Y. L. Jiang, and J. C. Blanks. 1996. Retinal light damage in rats with altered levels of rod outer segment docosahexaenoate. *Invest. Ophthalmol. Vis. Sci.* **37:** 2243–2257.
54. Toyokuni, S. 1999. Reactive oxygen species-induced molecular damage and its application in pathology. *Pathol. Int.* **49:** 91–102.
55. Awasthi, Y. C., Y. Yang, N. K. Tiwari, B. Patrick, A. Sharma, J. Li, and S. Awasthi. 2004. Regulation of 4-hydroxynonenal-mediated signaling by glutathione S-transferases. *Free Radic. Biol. Med.* **37:** 607–619.
56. Williams, C., E. E. Birch, P. M. Emmett, and K. Northstone. 2001. Stereoacuity at age 3.5 y in children born full-term is associated with prenatal and postnatal dietary factors: a report from a population-based cohort study. *Am. J. Clin. Nutr.* **73:** 316–322.
57. Weisinger, H. S., A. J. Vingrys, and A. J. Sinclair. 1996. Effect of dietary n-3 deficiency on the electroretinogram in the guinea pig. *Ann. Nutr. Metab.* **40:** 91–98.
58. Neuringer, M., W. E. Connor, D. S. Lin, G. J. Anderson, and L. Barstad. 1991. Dietary omega-3 fatty acids: effects on retinal lipid composition and function in primates. *In* Retinal Degenerations. R. E. Anderson, J. G. Hollyfield, and M. M. LaVail, editors. CRC Press, New York. 1–13.
59. Weisinger, H. S., J. A. Armitage, B. G. Jeffrey, D. C. Mitchell, T. Moriguchi, A. J. Sinclair, R. S. Weisinger, and N. Salem, Jr. 2002. Retinal sensitivity loss in third-generation n-3 PUFA-deficient rats. *Lipids.* **37:** 759–765.
60. Neuringer, M., W. E. Connor, D. S. Lin, L. Barstad, and S. Luck. 1986. Biochemical and functional effects of prenatal and postnatal omega 3 fatty acid deficiency on retina and brain in rhesus monkeys. *Proc. Natl. Acad. Sci. USA.* **83:** 4021–4025.
61. Diau Gy Fau - Loew E. R., Loew Er Fau - Wijendran V., Wijendran V. Fau - Sarkadi-Nagy E., Sarkadi-Nagy E. Fau - Nathanielsz P. W., Nathanielsz Pw Fau - Brenna J. T., Brenna J. T. Docosahexaenoic and arachidonic acid influence on preterm baboon retinal composition and function. (0146–0404 (Print)).
62. Hao, W., A. Wenzel, M. S. Obin, C. K. Chen, E. Brill, N. V. Krasnoperova, P. Eversole-Cire, Y. Kleyner, A. Taylor, M. I. Simon, et al. 2002. Evidence for two apoptotic pathways in light-induced retinal degeneration. *Nat. Genet.* **32:** 254–260.
63. Cho, E., S. Hung, W. C. Willett, D. Spiegelman, E. B. Rimm, J. M. Seddon, G. A. Colditz, and S. E. Hankinson. 2001. Prospective study of dietary fat and the risk of age-related macular degeneration. *Am. J. Clin. Nutr.* **73:** 209–218.
64. Seddon, J. M., J. Cote, and B. Rosner. 2003. Progression of age-related macular degeneration: association with dietary fat, transunsaturated fat, nuts, and fish intake. *Arch. Ophthalmol.* **121:** 1728–1737.
65. Crabb, J. W., M. Miyagi, X. Gu, K. Shadrach, K. A. West, H. Sakaguchi, M. Kamei, A. Hasan, L. Yan, M. E. Rayborn, et al. 2002. Drusen proteome analysis: an approach to the etiology of age-related macular degeneration. *Proc. Natl. Acad. Sci. USA.* **99:** 14682–14687.